TRANSLATIONAL CHEMISTRY
AN INTERFACE JOURNAL
HTTPS://WWW.TRANSLATIONALCHEMISTRY.COM/

REVIEW | DOI: 10.5584/translationalchemistry.v1i1.242

Translational Advances: Biomaterials and Antimicrobial Photodynamic Therapy, a Synergistic Approach

Filipe M. P. Morais[1,3], Carlos Lodeiro[2,3], Nuno M. M. Moura[1,*]

[1] LAQV-REQUIMTE, Department of Chemistry, University of Aveiro, 3810-193 Aveiro, Portugal. [2] PROTEOMASS Scientific Society, 2825-466, Sto Antonio de Caparica, Costa de Caparica, Portugal. [3] BIOSCOPE Research Group, LAQV-REQUINTE, Chemistry Department, NOVA School of Science and Technology, NOVA University Lisbon, 2829-516, Caparica, Portugal.

Received: April 2025 **Accepted:** May 2025 **Available Online**: June 2025

Abstract

The increasing prevalence of drug-resistant pathogens represents a serious public health challenge, driven by factors such as inadequate water sanitation, the misuse and overuse of antimicrobials, and insufficient infection prevention and control measures. Appropriately functionalized porphyrin derivatives present a promising strategy as broad-spectrum photo-antimicrobial agents, activated by visible light in the presence of molecular oxygen throughout photodynamic approach. These compounds effectively target resistant microorganisms, namely bacteria. To mitigate production costs, the immobilization of these compounds on solid supports has been proved essential, as it enables their recovery, reuse, and recycling. This approach enhances both the economic viability and environmental sustainability of antimicrobial photodynamic therapy. Furthermore, various biopolymers, including cyclodextrin, lignin and chitosan, have been employed to immobilize porphyrin-based photosensitizers, allowing for the tailoring of the substrates physicochemical and biological properties.

Keywords: Photosensitizers, porphyrins, photodynamic therapy, biopolymers, immobilization.

Introduction

Antimicrobial resistance is a major global health challenge that impacts individuals at all stages of life and has significant repercussions for healthcare, veterinary medicine, and agriculture. Key contributing factors include poor sanitation, limited access to clean water, inadequate infection prevention and control measures, and the improper use of antimicrobials. Consequently, there is an urgent need to create affordable and innovative treatments to combat drug-resistant pathogens [1–3]. Antimicrobial Photodynamic Therapy (aPDT) leverages the interaction of light, a photosensitizer (PS), and molecular oxygen to eliminate microorganisms. Upon absorbing light, the PS transitions to an excited state, initiating a series of energy transfers that ultimately leading to the generation of reactive oxygen species (ROS), namely singlet oxygen ($^1O_2$) [4,5]. These ROS are highly cytotoxic and effectively damage microbial cells. The process involves the PS absorbing light, moving through various excited states, and potentially undergoing intersystem crossing to a longer-lived triple state. This extended lifetime enhances energy transfer to molecular oxygen, leading to the generation of ROS. aPDT harnesses light to activate a PS, generating a targeted and localized oxidative attack against microorganisms [6–8]. This process oxidizes various cellular components, leading to rapid cell photoinactivation. aPDT offers advantages over traditional antimicrobials because it does not promote the development of resistance. Its ability to target multiple cellular sites, inflicting damage on various structures through ROS-induced oxidative stress, this extensive damage makes it difficult for microorganisms to develop resistance by altering a single target. Moreover, aPDT typically acts promptly, with microbial death occurring soon after treatment. This rapid action minimizes the selective pressure on microorganisms, unlike prolonged exposure to antibiotics, which provides more opportunities for resistant strains to emerge and multiply [4,5]. The effectiveness of photodynamic action in aPDT is largely determined by the structure of the PS and its capacity to generate ROS. Directing PS to specific subcellular locations, can amplify its phototoxic effects while minimizing harm to surrounding healthy tissues. The design of a PS also influences its biocompatibility and the likelihood of side effects. Ideally, a PS should exhibit minimal toxicity toward healthy cells while delivering potent cytotoxic effects to target cells. Although various organic compounds have been explored as PS in aPDT, porphyrins and related macrocycles are at the forefront of PS research. There is considerable interest in synthesizing

***Corresponding author:** Nuno M. M. Moura, E-mail: nmoura@ua.pt

porphyrins and their derivatives because of their unique properties, which are applicable in biomedicine, catalysis, and advanced materials. In the context of PS for aPDT, porphyrins exhibit distinctive characteristics such as chemical versatility, stability under light and during storage, strong absorption in the visible spectrum, efficient photoinduced reactions with molecular oxygen, low inherent toxicity, and a high binding affinity to cellular components such as membranes, proteins, and DNA [9–11]. The structure of the cell wall in Gram-positive and Gram-negative bacteria plays a crucial role in determining their sensitivity to aPDT. In general, PS molecules readily attach to Gram-positive bacteria, resulting in their photoinactivation. In contrast, Gram-negative bacteria tend to be more resistant to PS treatment due to their intricate cell wall structure. The presence of negatively charged lipopolysaccharides enhances the interactions with cationic PS, which can influence the treatment's overall effectiveness [12]. This review aims to provide a concise and comprehensive overview of recent advancements in the immobilization of porphyrin-based PS, particularly focusing on the use of various biopolymeric supports such as cyclodextrins, chitosan, and lignin, for developing cost-effective and environmentally friendly photoactive materials.

1. Preparation of cyclodextrin-porphyrin hybrids

Cyclodextrins (CD) are cyclic oligosaccharides composed of glucose units derived from starch through enzymatic conversion. The three most common types of CD are α (alpha), β (beta), and. γ (gamma), which consist of six, seven, and eight glucose units, respectively, arranged in a ring fashion (**Figure 1**). The central cavity of a CD molecule can encapsulate guest molecules, including hydrophobic substances such as neutral porphyrins, making them valuable for various applications. Additionally, these complexes can protect the encapsulated molecules from external environmental factors. One of the main fields application of CD is in the pharmaceutical field, where they enhance the solubility and stability of poorly water-soluble soluble drugs, thereby improving their effectiveness [13–15]. The use of CD in aPDT shows significant potential for improving the field by tackling important issues related to the formulation and delivery of PS [16,17].

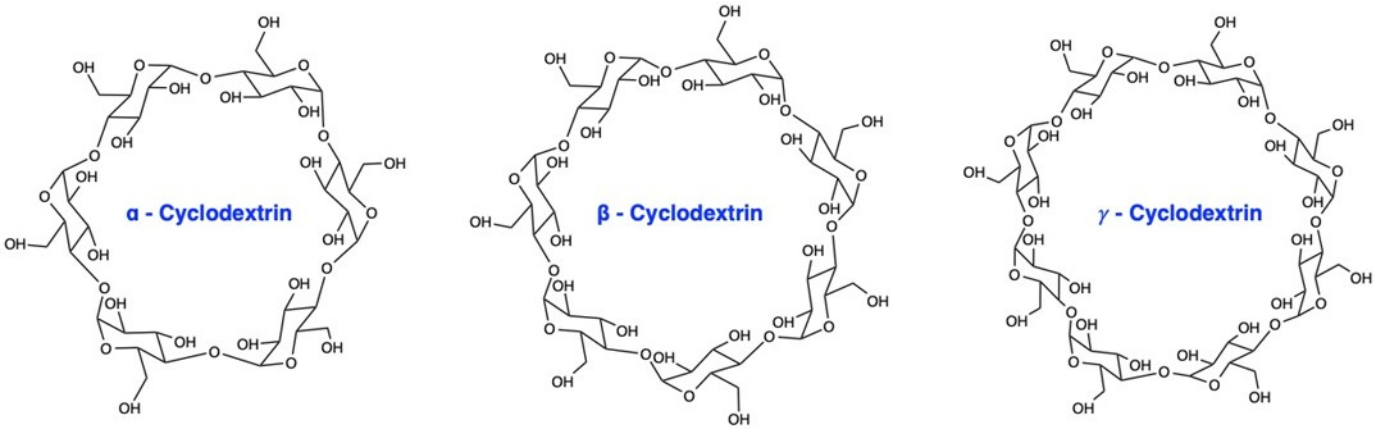

Figure 1 | Structures of α, β and γ cyclodextrins.

2.1. Covalent linkage

The covalent functionalization of porphyrin derivatives with CD can lead to the development of innovative molecular structures. Ribeiro *et al.* [18,19] synthesized two series of asymmetrical cationic free-base PS-CD conjugates containing α-, β- and γ-CD units (**Scheme 1**). The formation of PS-CD conjugates **4a–c** and **5a–c** involved the reaction of the appropriate neutral porphyrin bearing pyridone **1a** or thiopyridyl **1b** units with K_2CO_3 and α- or γ-CD in dry *N,N*-dimethylformamide (DMF) for 72 h at 60 °C under N_2 atmosphere, yielding the respective neutral porphyrin-CD conjugates **2a–c** and **3a–c** (41-58%). The neutral derivatives were submitted to a cationization reaction with a suitable alkylating agent. The tetracationic porphyrin derivatives bearing inverted methoxypyridinium units **4a–c** were obtained in yields ranging from 43 to 73%, while the corresponding thiopyridinium counterparts **5a–c** were isolated in better yields (70-95%) [18,19].

The photosensitizing properties of porphyrin-CD conjugates were assessed against *E. coli.* Overall, the thiopyridinium derivatives **5a–c** revealed a better performance and capability to photoinactivate the Gram-negative *E. coli*, exhibiting a strong correlation between the $^1O_2$ generation capability and the aPDT efficiency. Porphyrin-CD conjugate **5c** exhibited the best performance reaching the limit detection of the method at a concentration of 5.0 μM after 15 min at an irradiance of 25.0 mW/cm^2, while the α-CD counterpart **5a** required 30 min of irradiation under the same conditions. Porphyrin-CD conjugates **4a–c** bearing methoxypyridinium units experienced a poor photodynamic effect at an irradiance of 25.0 mW/cm^2, have been observed only ≈ 1.5 Log reduction in the viability of *E. coli* by derivative **4c**. An irradiance enhancement to 50.0 mW/cm^2 led to a better performance for this series of porphyrin-CD conjugates being observed a ≈ 4.0 Log reduction in the viability of *E. coli* in the presence of **4c** and ≈ 3.0 Log with **4a** and **4b** after 60 min of irradiation [18,19].

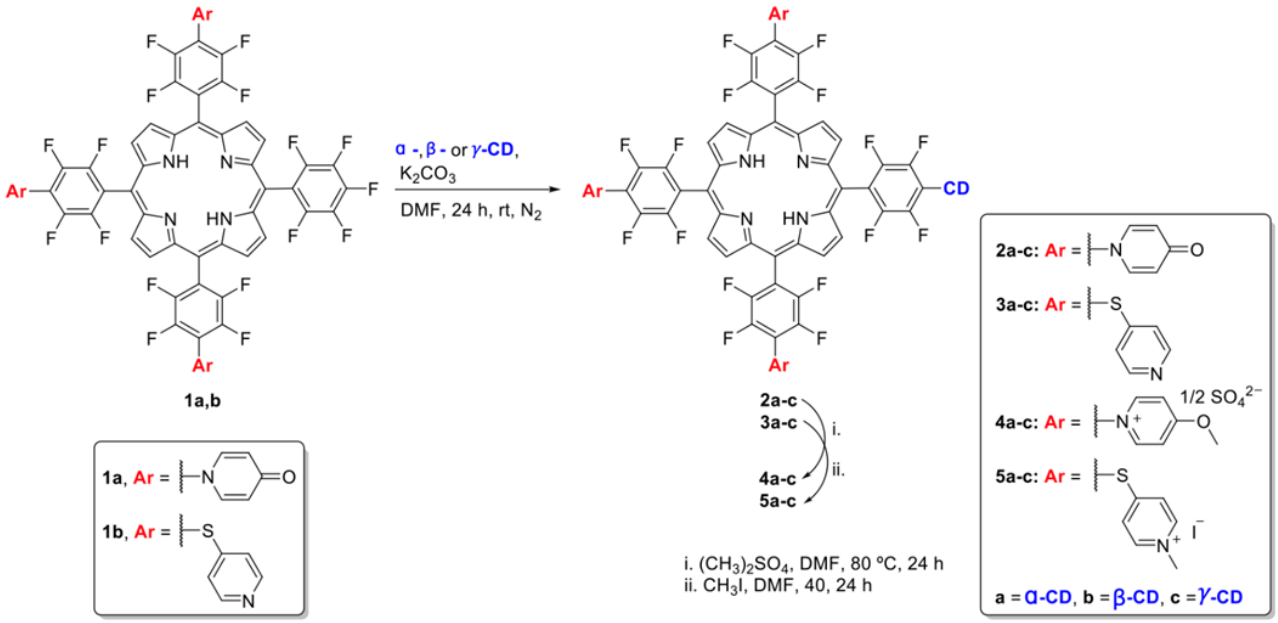

Scheme 1 | Synthetic approach to prepare cationic porphyrin-CD conjugates **4a–c** and **5a–c** prepared by C.P.S. Ribeiro *et. al.* [18,19].

aPDT assays showed the relevance of the capability of porphyrin derivatives to generate $^1O_2$ as well as the position of the positive charge to provide porphyrin-CD-based PS with improved capability to photoinactivate *E. coli.* The positive charge at an external position of the thiopyridinium units of porphyrin-CD conjugates **5a–c** probably enhanced the interaction between the PS and the bacterial membrane enhancing the aPDT effect, while for derivatives **4a–c** the inverted position of the methoxypyridinium hindered this interaction. Additionally, the CD cavity size also seems to play a relevant role in the aPDT effect, being the γ-CD preferable compared to α- and β-CD.

Continuous efforts have been made to synthesize CD-based conjugates modified with porphyrin PS to that effectively respond to light. In this context, Panagiotakis *et al.* [20] synthesized porphyrin β-CD conjugates **7a–c** via amide bond coupling. The process involved reacting mono-(6-amino-deoxy)-β-CD with 5-[4 (4-carboxyalkyloxy)phenyl]-10,15,20-triphenylporphyrins, which differed in alkyl chain lengths (**Scheme 2**).

The adequate porphyrin **6a–c** was reacted with amino-functionalized β-CD in the presence of 4-(4,6-dimethoxy-1,3,5-triazin-2-yl)-4-methyl-morpholinium chloride (DMTMM) and *N,N*-diisopropylethylamie (DIPEA) in DMF and under N_2 atmosphere at room temperature for 24 h. After chromatographic purification and dialyzes approach, the porphyrin-β-CD conjugates **7a–c** was obtained as dark brown solids with yields ranging from 56% (**7a**) to 94% (**7c**). Conjugates **7a–c** exhibited the capability to produce $^1O_2$, a key factor for aPDT applications, when irradiated in PBS [20].

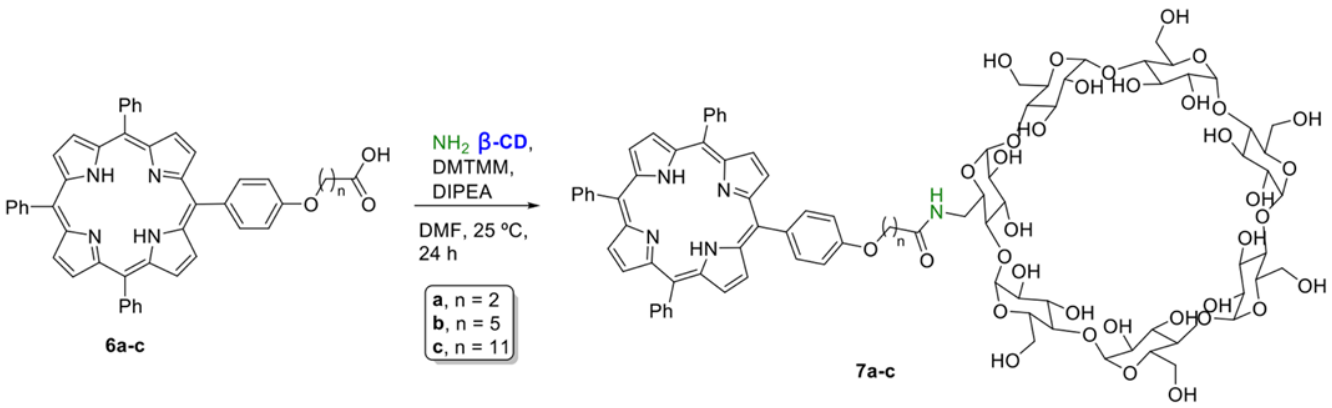

Scheme 2 | Synthesis of porphyrin-CD conjugates **7a–c** prepared by S. Panagiotakis *et. al.* [20].

2.2. Supramolecular interaction

The non-covalent interaction between β-CD and porphyrins provides a practical and flexible method for exploring the photophysical and photochemical properties of porphyrins. Additionally, this interaction facilitates the creation of functionalized supramolecular assemblies in water. Yu *et al.* [21] prepared the porphyrin-β-CD conjugate **9** through non-covalent interactions β-CD-factionalized1,8-naphthalimide-based derivative **8** with 5,10,15,20-tetra(4-sulfonatophenyl)porphyrin (**TPPS$_4$**) (**Scheme 3**). This approach involved the previous functionalization of 1,8-naphthalimide core with an excess of permethyl-β-CD under typical Click-chemistry reaction conditions to afford derivative **8**. Then, by taking advantage of the strong binding interactions between the tetraanionic porphyrin derivative **TPPS$_4$** and the β-CD cavity, the supramolecular assembly was carried out by combining both components in an aqueous solution. In this process, the porphyrin effectively entered the non-polar cavity of CD through Van der Waals interactions, which served as the main binding force and also prevented the self-aggregation of porphyrin [21].

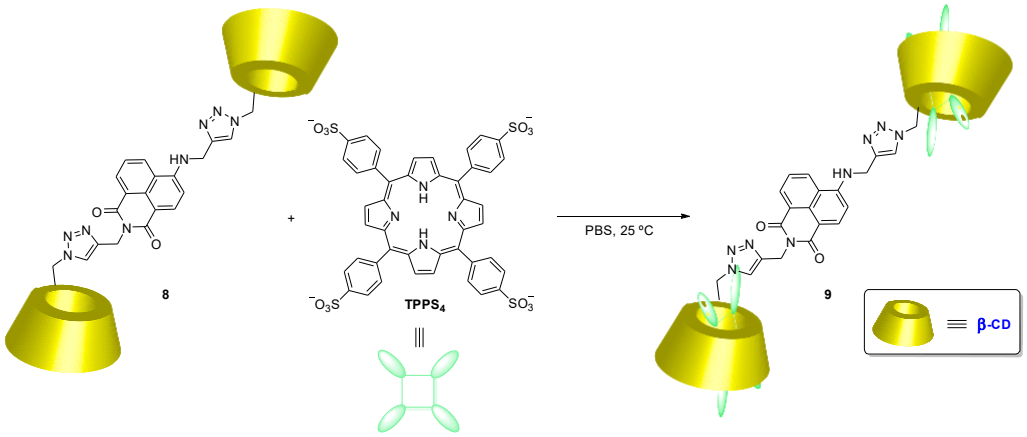

Scheme 3 | Schematic preparation of porphyrin-β-CD conjugate **9** synthesized by Yu *et al.* [21].

Nanoformulations in drug delivery systems provide significant advantages over traditional treatment methods, including reduced drug toxicity and side effects, improved bioavailability, and sustained drug release at infection sides. Choi *et al.* [22] developed a β-CD formulation incorporating the gallium(III) complex of 5,10,15,20-tetraphenylporphyrin (**TPP**). The preparation of the **CD-GaTPP** conjugate took place in a 10 mM HEPES buffer solution using gallium(III) **TPP** and β-CD through a homogenization technique at room temperature with overnight stirring. The resulting mixture was then sonicated on ice, followed by washing with distilled water and reconstituted in PBS [22].

The use of nanophototherapeutics-based drug delivery system is seen as an effective way to improve the targeted release of PS while reducing the risk of unwanted photosensitization from PS buildup in healthy tissues [23]. Zagami *et al.* [24] developed nanoassemblies by mixing CAPTISOL® (sulfobutylether-β-cyclodextrin) and 5,10,15,20-tetrakis(1-methylpyridinium-4-yl)porphyrin (**TMPyP**) in a 1:1 molar ratio and stirred magnetically at room temperature for 10 min. (**Figure 2**).

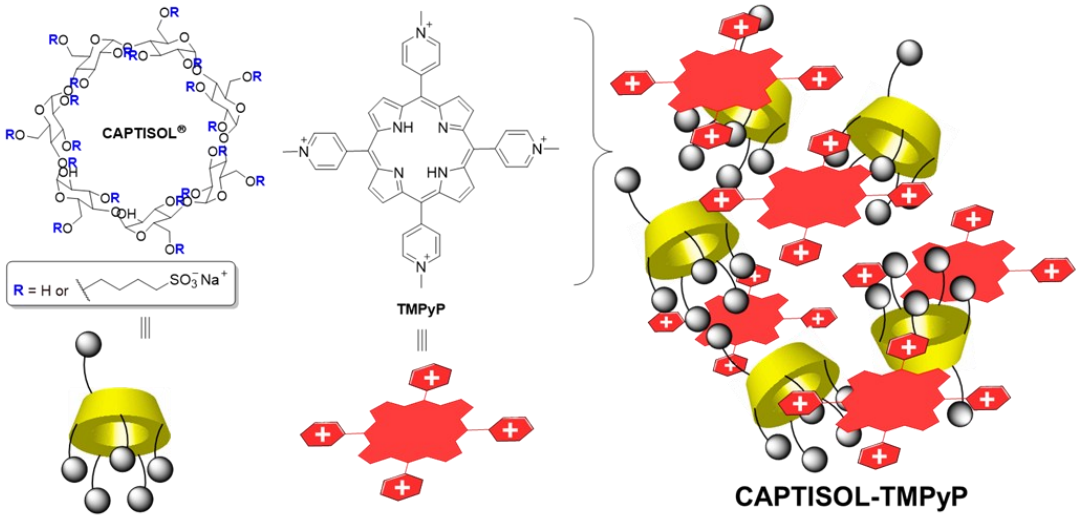

Figure 2 | Outlined depiction of the preparation process for CAPTISOL-**TMPyP** nanoassembly considered in the work by by Zagami *et al.* [24].

These innovative nanoformulations not only showed improved PS stability and controlled release but also maintained strong aPDT activity against *P. aeruginosa*, *E. coli*, and *S. aureus*, all at a PS concentration of 6.0 μM and a light dose of 42.0 J/cm^2 against both Gram-positive and Gram-negative bacterial cells. This research highlights the promise of CD-based nanocarriers in enhancing the therapeutic effectiveness of aPDT [24].

The same group studied a different nanoformulation with a CAPTISOL-**TMPyP** ratio of 50:1. A series of aPDT assays were performed using **TMPyP** at a 1:50 molar ratio. Notably, this nanosystem demonstrated strong photo-bactericidal activity against both Gram-positive and Gram-negative bacteria with Minimum Inhibitory Concentration (MIC) of 3 μM and 6 μM, respectively. Interesting results were observed in experiments with *P. aeruginosa*, showing that CAPTISOL alone can inhibit the production of pyocyanin, an important virulence factor, while also affecting bacterial biofilm formation. This effect is likely due to the quorum quenching mechanism of CD, which interferes with bacterial communication among Gram-negative strains. When paired with **TMPyP**, CAPTISOL demonstrated a synergetic effect, leading to both the inhibition and destruction of *P. aeruginosa* biofilm formation [25]. Later, Zagami *et al.* [26] prepared a three-dimensional network CD-based nanosponges (NS) through a cross-linked approach with pyromellitic dianhydride (PMDA) (**Scheme 4**). The preparation of the NS doped with **TMPyP** required the previous preparation of the **PMDAβ-CD** NS by mixing β-CD and PMDA in 8:1 ratio in dimethyl sulfoxide (DMSO) in the presence of triethylamine at room temperature and under vigorous stirring. The obtained NS was then mixed with **TMPyP** using a mass ratio of 25:1. The resulting dispersion was stirred magnetically for 3 h at room temperature to obtain the **PMDAβ-CD-TMPyP** conjugate. It was observed that NS protects **TMPyP** from photodegradation rather than controlling its release throughout the treatment period. Also, the incorporation of **TMPyP** do not compromise its capability to generate $^1O_2$, since **PMDAβ-CD-TMPyP** conjugate exhibits comparable to ϕΔ that of free **TMPyP** (0.67 *vs* 0.74) [26].

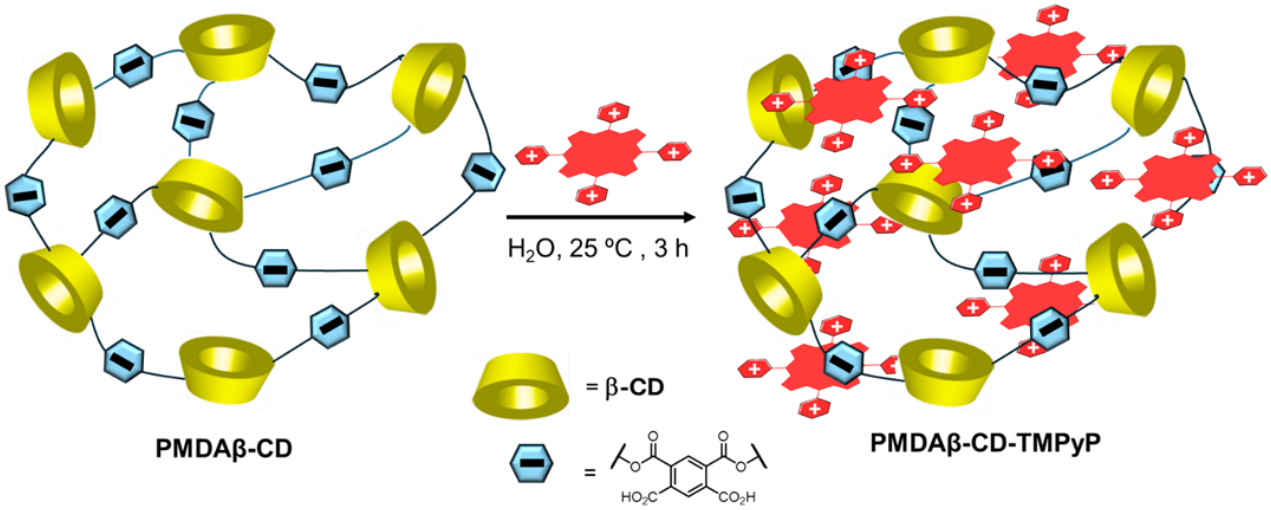

Scheme 4 | Schematic representation of the synthetic approach to prepare the NS **PMDAβ-CD-TMPyP** conjugate developed by Zagami *et al.* [26].

Biological assays were performed to assess the photobacterial activity of both **TMPyP** and **PMDAβ-CD-TMPyP** conjugate against *P. aeruginosa* and *S. aureus* at a PS concentration of 3.75 μM. It was achieved a complete reduction in bacterial load for both strains. However, while free **TMPyP** reached the bacterial full photoinactivation after just 1 h with a total light dose of 13.71 J/cm^2, the **PMDAβ-CD-TMPyP** NS required 4 h of light exposure (54.82 J/cm^2) [26].

Meso-tetraarylporphyrins bearing hydroxyphenyl (**10a,b**) or dihydroxyphenyl (**10c,d**) moieties were successfully encapsulated with two trimethyl-β-CD (**TMeβ-CD**) units (**Scheme 5**). The formation of the porphyrin-CD supramolecular structure enabled the solubility in water of the porphyrin derivatives eliminating the need for further chemical modifications on the porphyrin core or the use of co-solvents (e.g. DMSO) (**Scheme 5**). The supramolecular porphyrin-**TMeβ-CD** conjugates **11a–d** were prepared by mixing both components using mechanochemical high-speed vibration-milling (HSVM) technique for 20 min. After this period, the solid mixture was suspended in pure water, following removal of non-encapsulated porphyrin derivatives through centrifugation. All porphyrin derivatives linked with CD successfully generated $^1O_2$ [14,27].

Xia *et al.* [28] developed a supramolecular porphyrin-CD PS through host-guest and assembling of the tetra-substituted porphyrin-triazolyladamantane derivative **12** with a dimer of permethyl-β-cyclodextrin (**Scheme 6**). Both components were dissolved in a DMSO/H_2O mixture (3:7) and stirred at room temperature form 12 h, followed by dialysis to remove DMSO to afford **12**-CD Conjugate in a 1.33 mg/mL concentration. The supramolecular complex **12**-CD demonstrated significant effectiveness in producing $^1O_2$. These results highlight the potential of the complex as a promising candidate for aPDT [28,29].

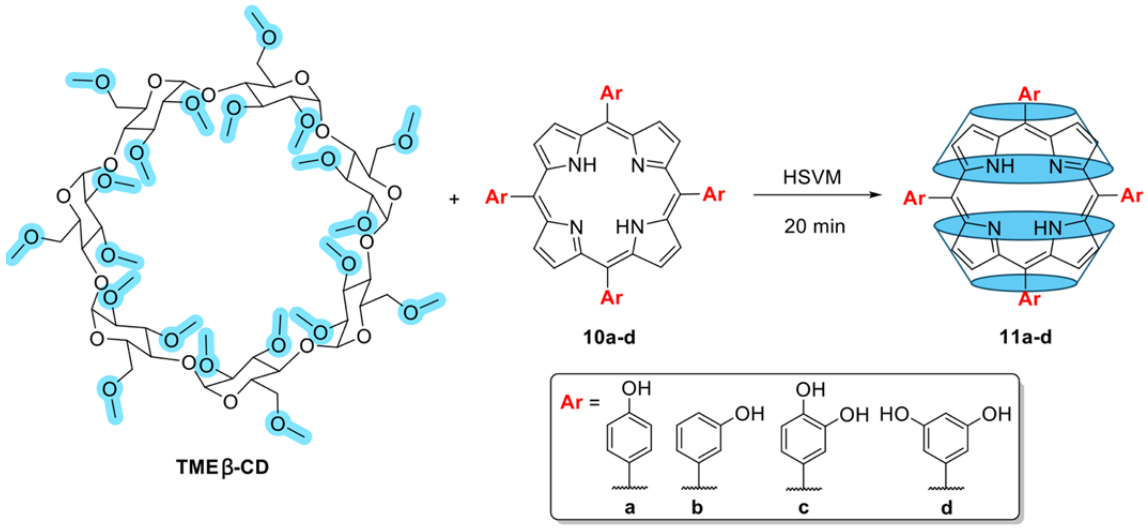

Scheme 5 | Schematic preparation of porphyrin-TMEβ-CD conjugates **11a–d** considered in the work of Ikeda and co-workers [14,27].

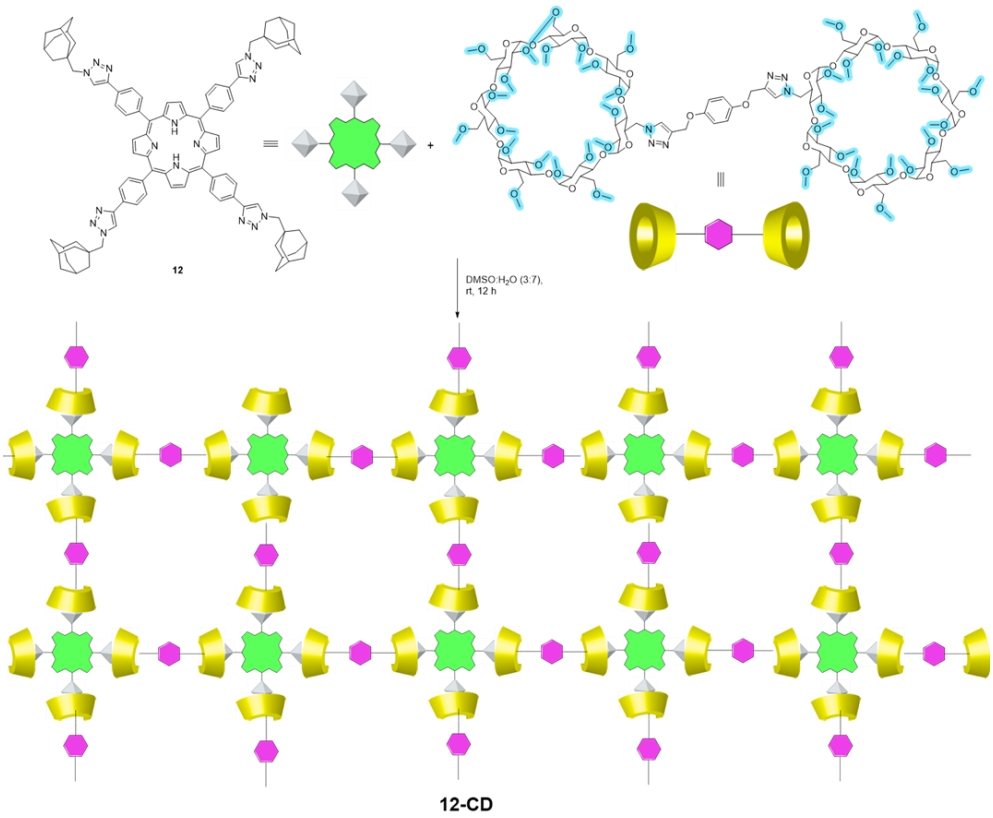

Scheme 6 | Schematic representation to prepare **12**-CD conjugate synthesized by Xia *et al.* [28].

3. Chitosan

Chitosan (CS) is a naturally occurring polysaccharide derived from the deacetylation of chitin, composed mainly of β-(1→4) linked D-glucosamine and *N*-acetyl-D-glucosamine. Its molecular structure features free amino groups that enhance solubility under acidic conditions and contribute to its mucoadhesive and antimicrobial properties. This polysaccharide is present in the shells of crustaceans and also found in the exoskeletons of insects and the cell walls of certain fungi [30,31]. CS degree of deacetylation and molecular weight can be adjusted to tailor its functional properties. This versatility makes it a promising material for various biomedical and industrial applications, including drug delivery systems, wound healing scaffolds, and tissue engineering [30,32,33]. In photodynamic approaches, CS biocompatibility, biodegradability, and mucoadhesiveness have been leveraged to develop NPs-based delivery systems that improve the stability, bioavailability, and targeted uptake of PS [34]. Chemical modifications such as acylation, alkylation, and esterification have further enhanced its solubility, mechanical strength, and drug-

release profiles, while its intrinsic antimicrobial activity synergistically enhance the therapeutic effects in combating infections. Additionally, it is cost-effective and environmentally friendly, posing no threat to the ecosystem [35,36].

Castro *et al.* [37] prepared a series of CS-based films modified with different *meso*-tetraarylporphyrins aiming to taking advantage of CS antimicrobial and film forming features. Porphyrin derivatives bearing carboxylic acid units were selected to be immobilized in CS to improve the electrostatic interactions with the CS amino units. and 5,10,15,20-tetrakis(4-carboxyphenyl)porphyrin (**TCPP**) and 5,10,15,20-tetrakis(pentafluorophenyl)porphyrin (**TPFPP**) were prepared through well-described approaches. **TPFPP** was further used as a scaffold to prepare the corresponding thio-carboxylate derivatives **13a,b** through nucleophilic aromatic substitution of the *p*-fluorine atoms in **TPFPP** with 3- and 4-mercaptobenzoic acid (**Figure 3**).

For the immobilization of porphyrin derivatives within a chitosan matrix, a chitosan solution was slowly added dropwise to the porphyrin solution in acetone, while continuously stirring magnetically. The resulting matrix was stirred in the dark for 72 h at room temperature, allowing for the complete evaporation of acetone to obtain the **porphyrin@CS** hybrid. **TPFPP** exhibited an immobilization rate in CS of 16%, while it was significantly improved for **TCPP** and **13a,b** reaching a porphyrin immobilization rate ranging from 76% (**TCPP**) to 100% (**13a**). This data confirms the relevance of the presence of the carboxylic acid units to enhance the interaction with the CS matrix. The **porphyrin@CS** films exhibited photostability and were effective in generating $^1O_2$. Additionally, **TCPP** attachment to CS reduced the aggregation-induced quenching of $^1O_2$ production observed for the free counterpart in solution. The **porphyrin@CS** films displayed anti-adherent characteristics, successfully preventing cell attachment and biofilm formation of *Listeria innocua*.

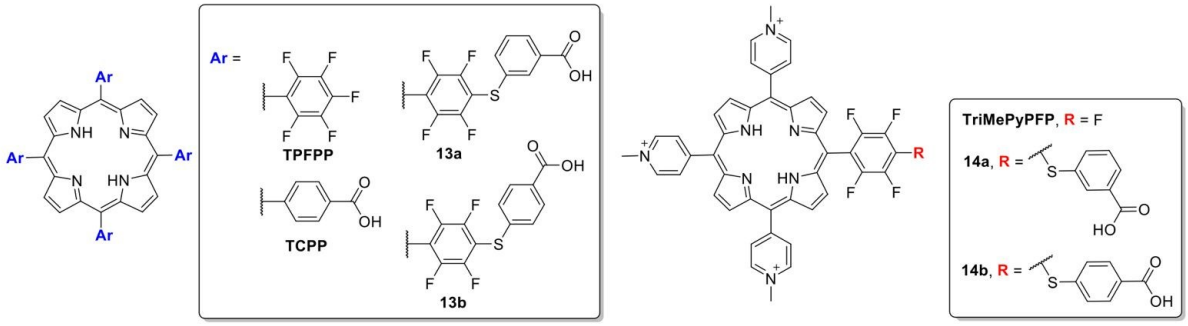

Figure 3 | Structures of porphyrin derivatives used by Castro *et al.* to prepare different CS-based films [37].

This property is dependent on the porphyrin structure and the $^1O_2$ generation capability of CS films, and the combination of photodynamic inactivation and biofilm prevention makes these materials strong contenders of antifouling coatings, especially in the food industry. The study emphasizes how the structure of porphyrins plays a vital role in influencing the overall aPDT of the CS based materials [37].

In a separate study, Silva *et al* studied the photodynamic activity of **13b@CS** films against cancer cells. The incorporation of **13b** into chitosan nanostructures mitigates aggregation issues associated with non-incorporated **13b** and enhances the photosensitizing properties of **13b@CS** by 3-fold compared to free **13b** in HeLa cells [38].

Based on previous results, the same research group studied the immobilization of two tricationic porphyrin derivatives (**14a,b**) featuring a thio-carboxylate units and their precursor **TriMePyPFP** in CS. Then, was assessed the aPDT effectiveness of both **TriMePyPFP@CS** and **14@CS** films towards the bioluminescent Gram-negative *Escherichia coli* bacterium. The results showed that the position of the carboxyl group in the mercapto units or the absence of these substituents in the porphyrin macrocycle modulate the action of the PS against *E. coli*. Porphyrin **14a,b** after incorporated in CS films, exhibited a poor capability to generate $^1O_2$ which is strongly correlated with their lack of aPDT effect. After 90 min of exposure to light, only **TriMePyPFP@CS** was able to induce a ≈ 4 Log reduction in the viability of *E. coli* [33].

Zhang *et al.* [39] developed an advanced antimicrobial system by incorporating **Fe-TCPP** NPs into CS. This system leverages the electrostatic targeting of CS in conjugation with aPDT. **TCPP** was coordinated with Fe_3O_2 clusters, forming **Fe-TCPP** NPs (**Scheme 7**). Then, **Fe-TCPP** NPs were encapsulated into a CS matrix. The **Fe-TCPP@CS** nanocomposite were able to induce substantial reduction in 9,10-anthracenediyl-bis(methylene)dimalonic acid (ABDA) absorbance upon light exposure, indicating a strong capacity for ROS production [39].

The efficacy of **Fe-TCPP@CS** was evaluated against both Gram-positive *S. aureus* and Gram-negative *E. coli* bacterial strains. Upon exposure to white light (0.3 W/cm^2, 10 min) at a concentration of 20 μg/mL, was able to induce a 97% reduction in the viability of *S. aureus*. However, **Fe-TCPP@CS** nanocomposite was much less effective against *E. coli*. Even after a ten-fold increase in the PS concentration, it only reached a bacterium photoinactivation lower

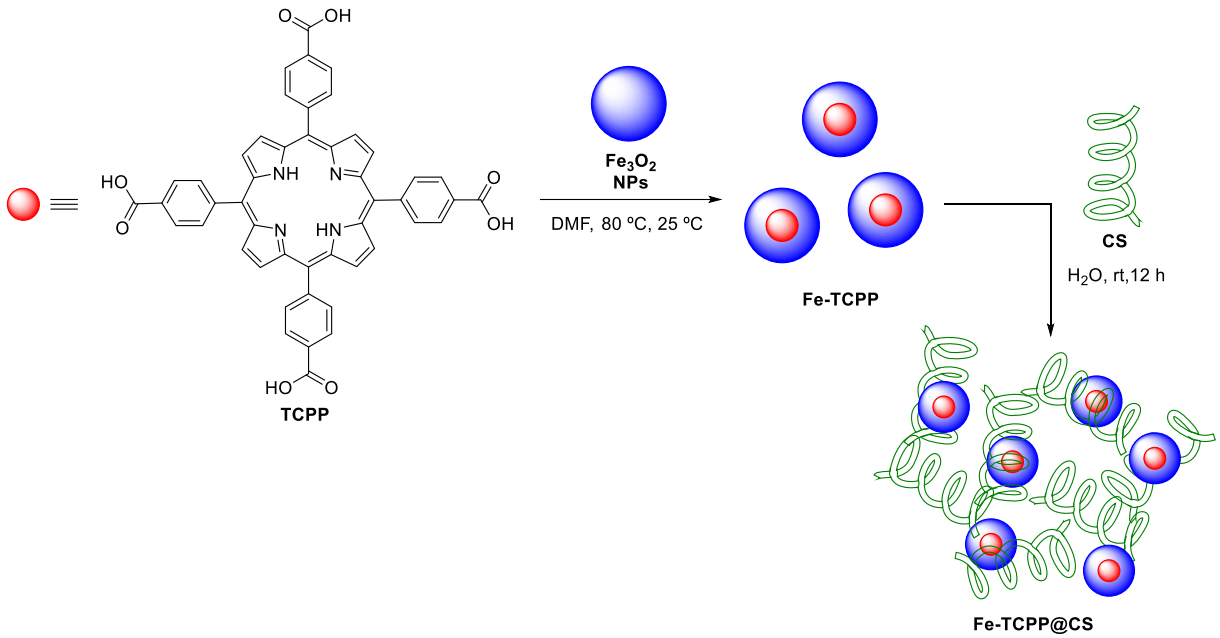

Scheme 7 | Schematic representation depicting the synthesis approach used to prepare **Fe-TCPP@CS** nanocomposite by Zhang *et al.* [39].

than 50%. To enhance efficacy against *E. coli*, the researchers investigated a synergetic approach combining aPDT with photothermal therapy. This combined strategy achieved approximately 98% elimination of *E. coli* at a concentration of 100 μg/mL under 635 nm laser irradiation (1.0 Wcm^2, 10 min). The $^1O_2$ generation capability of **Fe-TCPP@CS** nanocomposite highlights their potential as a promising candidates for advancing aPDT in the treatment of bacterial infections through a combined synergetic effect with photothermal therapy [39].

Hasanin *et al.* [40] investigated the potential of 5,10,15,20-tetrakis(3 -hydroxyphenyl)porphyrin (**10b**) loaded onto an CS and ethyl cellulose (EC)-CS nanocomposites, activated by laser irradiation, for combating multidrug-resistant bacteria (**Figure 4**) [40]. Laser irradiation of free **10b** in the blue region (70 mW, 15 min) resulted in a significant reduction in microbial survival rates. The **10b@CS** nanocomposite exhibited a slightly reduced efficacy under identical blue light irradiation conditions. However, the incorporation into EC-CS biopolymeric matrix not only retained the photodynamic activity of **10b** but also enhanced its physicochemical properties, particularly the absorption in the therapeutic red region (635 nm). The **10b@CE-CS** nanocomposite demonstrated remarkable reductions in microbial survivals rates upon exposure to 635 nm laser light (5.0 mW/cm^2, 15 min), highlighting its potential as a highly effective therapeutic agent [40].

Introducing diamagnetic heavy metal ions into the porphyrin cavity significantly fine-tune its photophysical and photochemical properties, typically leading to an increase in the $^1O_2$ production capability through enhanced intersystem crossing compared to the corresponding free-base counterpart [41,42]. Sen *et al.* [43] prepared a series of **porphyrin@CS** nanocomposites **15a–c** through

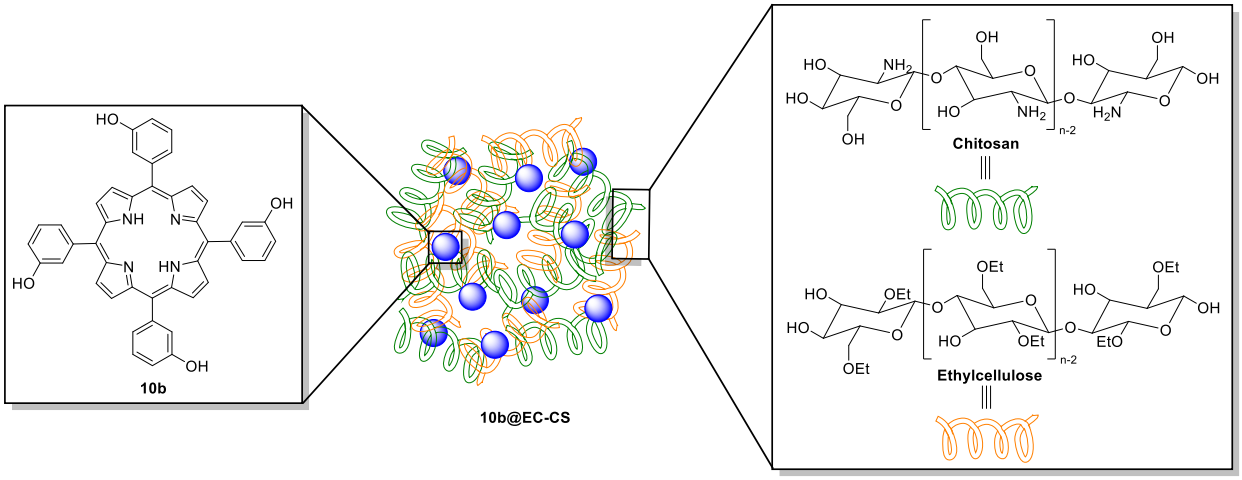

Figure 4 | Schematic representation of **10b@EC-CS** nanocomposite used in the work of Hasanin *et al.* [40].

the incorporation of 5,10,15,20-tetrakis(4-dibutylaminophenyl) porphyrin **15a** and their neutral and tetracationic Pd(II) complexes **15b,c** into CS. As expected the incorporation of the heavy metal Pd(II), have been the CS-based nanocomposite prepared with the tetracationic metalloporphyrin **15c** those with the highest efficiency in the generation of the cytotoxic species $^1O_2$ [43].

The authors assessed the photo-antimicrobial properties of the **porphyrin@CS** nanocomposites against *S. aureus*, focusing on the impact of Pd(II) ion, molecular charge, and CS conjugation on aPDT efficiency (**Figure 5A-C**) [43]. The tetracationic metalloporphyrin **15c** and their CS conjugate demonstrated better photoinactivation activity, even at low PS concentration (0.5 μM), reaching the full photoinactivation of *S. aureus* after 15 min of irradiation. Meanwhile the non-embedded counterpart required 30 min of irradiation under the same conditions to achieve identical results (**Figure 5C**). These results highlighted the best performance of the **porphyrin@CS** conjugates which can be attributed to the synergetic antibacterial properties of CS, which contribute to an amplified photoinactivation effect. Nonetheless, the improved activity also inducing some dark toxicity. The poor effectiveness of the neutral derivatives **15a,b** is mainly related to their propensity for aggregation in aqueous media, which compromises aPDT effect [43].

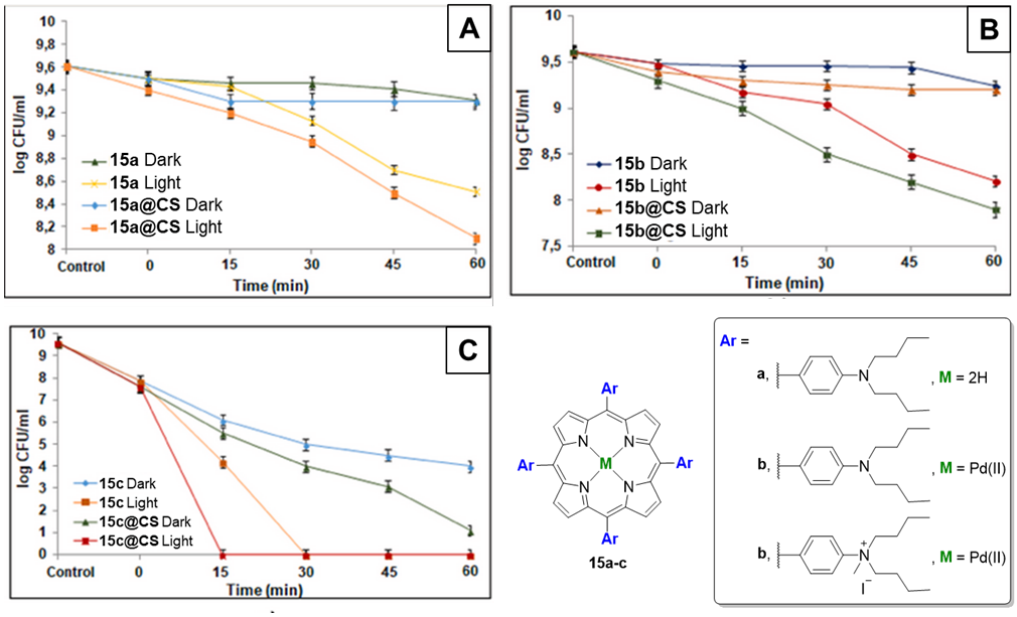

Figure 5 | Evaluation of the photo-antimicrobial activity of **porphyrin@CS** hybrids against *S. aureus*. Adapted from reference [43]

4. Lignin

Lignin (Li) is a complex, aromatic and heterogeneous organic polymer that constitutes a key component of plant cell walls, providing structural integrity and resistance against environmental stresses. Although it is most abundant in wood, lignin is also present in other plant tissues such as bark and fibers [44,45]. Chemically, lignin is a phenolic polymer with a highly variable structure, formed through the polymerization of phenolic monomers such a coniferyl, sinapyl, and *p*-coumaryl alcohol. The specific composition and linkage patterns of these monomers differ among plant species. Beyond its various industrial applications, lignin has attracted considerable interest as a renewable and sustainable resource. Researchers have been investigated its potential for producing biofuels and other value-added products, which could contribute to the advancement of a sustainable bioeconomy [46,47].

Despite its natural abundance, Li has historically received limited attention for photodynamic therapy applications, mainly due to its inherent antioxidant properties. Recently, however, lignin has emerged as a promising material in PDT research. Researchers have been exploring lignin-based NPs as delivery vehicles for PS, aiming to enhance their delivery and improve therapeutic efficacy. These lignin-based nanocarriers offer notable benefits, including biocompatibility, biodegradability, and the potential for targeted tissue delivery [48].

Carmona *et al.* [49] employed a multi-step procedure to encapsulate 5,10,15,20-tetrakis(4-hydroxyphenyl)porphyrin (**10a**) within acetylated lignin (AcLi) to obtain **10a@AcLi** NPs (**Scheme 11**). This approach involved the previous acetylation of Li by reacting a kraft lignin with acetic anhydride and dry pyridine 1:1 mixture at room temperature for 48 h. To obtain **10a@AcLi** hybrids, a **10a** and AcLi mixture was prepared in acetone, following by 24 h dialysis against water and 1 h centrifugation (**Figure 6**). **10a@AcLi** NPs exhibited high stability, with minimal **10a** leakage (9%) and both **10a@AcLi** and the non-encapsulated porphyrin counterpart AcLi demonstrated $^1O_2$ production after 30 minutes of irradiation [49].

The authors assessed the potential of **10a@AcLi** as PS against several bacterial strains of both Gram-positive and Gram-negative bacteria (**Figure 6**) [49]. The study evaluated the aPDT effect of **10a@AcLi** NPs and found out that they were quite effective against Gram-positive bacteria, achieving 99.9% reduction in survival at concentrations below 5 μM when exposed to low doses of white LED light (4.16 J/cm^2, 1 h irradiation). However, under the same irradiation conditions did not show noticeable impact on Gram-negative bacteria. The study suggests that the reason for the lack of effectiveness against Gram-negative bacteria might be due to the impermeability of their cell walls to the nanoparticles. TEM observations showed that **10a@AcLi** remained outside the bacterial cells, affecting the cell wall and causing flocculation (**Figure 6**).

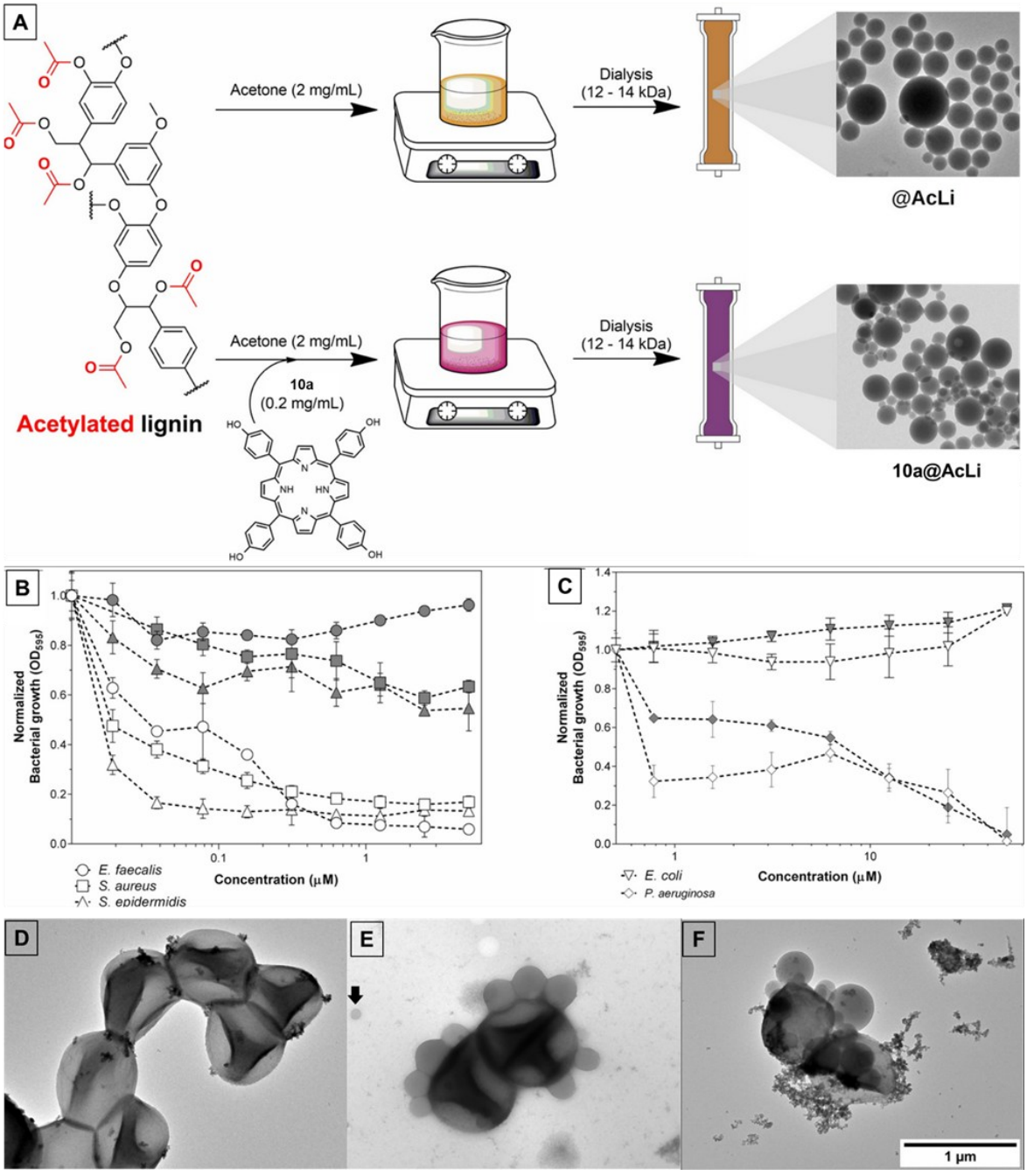

Figure 6 | **A**) Preparation of acetylated lignin-based **@AcLI** and **10a@AcLi** NPs. Bacteriostatic effect of **10a@AcLi** NPs after light irradiation (white LED light dose, 4.16 Jcm^2, white symbols) or dark incubation (gray symbols) against **B)** three Gram-positive bacteria and **C)** two Gram-negative bacteria. Transmission electron microscopy (TEM) observations of **D**) *S. aureus* cells in vivo; **E**) *S. aureus* and **10a@AcLi**, the black arrow indicates a non-bound nanoparticle; and **F**) *S. aureus* and **10a@AcLi** after light irradiation (incandescent bulb, 2.500 luxes, 5 min). Adapted from reference [49]

The same group followed an analogous protocol to incorporate a series of neutral and cationic free-base porphyrin derivatives **16a–c** and the Zn(II) complex **17** (**Figure 7**) to prepare other **porphyrin@AcLi** NPs to explore structure-activity relationship [50,51]. The **porphyrin@AcLi** NPs follows similar trends for both $^1O_2$ generation capability and fluorescence quantum yield as follows **16c@AcLi** > **16a@AcLi** > **16b@AcLi** > **10a@AcLi** > **17@AcLi** [49,51]. This study revealed the higher relevance of the pyridinium units to provide better performance in both properties.

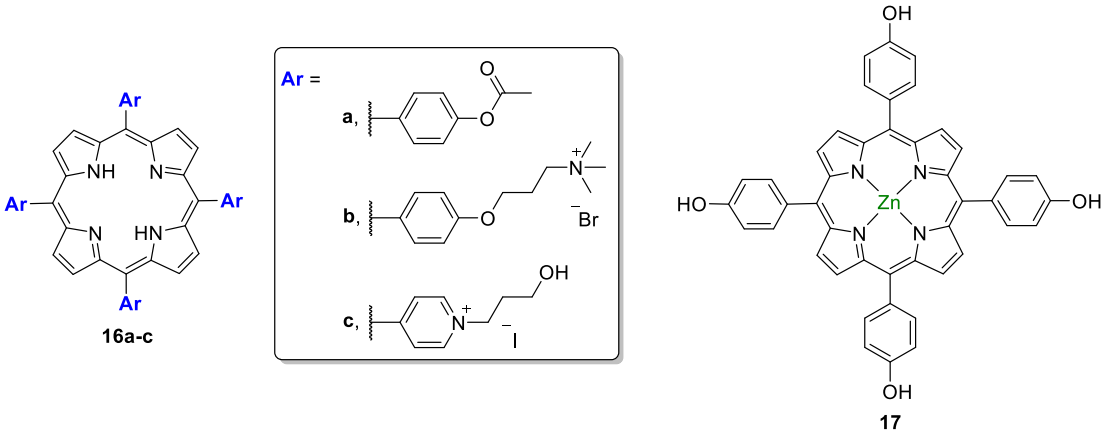

Figure 7 | Chemical structures of free-base porphyrin derivatives **16a–c** and Zn(II) complex **17** incorporated into AcLi NPs by Carmona *et al.* [50,51].

The photo-antimicrobial properties of **porphyrin@AcLi** NPs were further evaluated against *S. aureus* and *E. coli*. Their previous findings have established the efficacy of **10a@AcLi** in eradicating Gram-positive bacteria under white LED light exposure (4.16 J/cm^2, 1 h irradiation). The minimal bactericidal concentrations (MBC) for Gram-positive bacteria were lower, with effective aPDT results at 2.5 μM of **10a@AcLi**. However, even when **10a@AcLi** was used at a concentration of 50 μM, it was not able to induce a reduction in the viability of Gram-negative bacteria under the same irradiation conditions. This emphasizes how **10a@AcLi** was selective against Gram-positive bacteria while falling against Gram-negative bacterial strains [49]. The aPDT effect of **10a@AcLi**, **16a–c@AcLi** and **17@AcLi** NPs and the corresponding non-encapsulated porphyrin was further assessed against *S. aureus* and *E. coli* upon exposure to blue LED light (455 ± 5 nm, 15.0 J/cm^2, 30 min). While encapsulation generally led to a decrease in light-dependent antibacterial activity, for example compound **10a** showed a light activated MBC of 0.0488 μM, while **10a@AcLi** was 0.7813 μM against *S. aureus*, it conferred a significant advantage by minimizing dark toxicity, for example compound **17** showed dark toxicity at around 0.3 μM against *S. aureus*, whereas compound **17@AcLi** showed no effect at 50 μM. Notably, the encapsulation of the lipophilic porphyrin **16a**, which was inactive in its free form (>50 μM MBC against *S. aureus*), enhanced its bactericidal efficacy when encapsulated (**16a@AcLi** showed ≈ 2.5 log reduction at 12.5 μM). The mechanism of action for the encapsulated porphyrins appears to involve localized generation of ROS at the bacterial surface. For *E. coli*, free cationic porphyrins like **16b,c** exhibited greater activity, and the impact of encapsulation on their efficacy varied significantly [51]. Tse *et al.* [52] developed a one-pot synthetic strategy to synthesize sustainable lignin NPs decorated with porphyrin moieties. Lignin-based NPs **19@Li** were prepared under mild reaction conditions through a typical 5-5' linkage interunit azo-coupling between porphyrin **17** and alkali lignin (AL) (**Scheme 8**). Porphyrin **19** was previously prepared via a two-step approach from 5,10,15,20-tetrakis(4-aminophenyl)porphyrin **18** involving the sequential preparation of the corresponding diazonium salt then underwent a one-pot coupling reaction with 2-phenylphenol yielding the diazonium-porphyrin **19**. **19@Li** NPs exhibited capability to generate $^1O_2$ ($\phi\Delta$ = 0.62) and robust photostability, thereby underscoring their potential application in PDT [52].

Concluding remarks

The growing threat posed by drug-resistant pathogens is prompting a reevaluation of antimicrobial strategies. In this context, aPDT using PS like porphyrin derivatives is emerging as a promising approach. To make aPDT more practical and cost-effective, researchers are exploring methods to attach PS to solid supports for efficient recovery and reuse. Various biopolymeric matrixes, such as CD, CS and Li, are being investigated for this purpose, each offering unique advantages in terms of stability, targeted delivery, and overall effectiveness. Additionally these materials are readily accessible and biocompatible, contributing to the cost-effectiveness and environmentally friendliness of aPDT approach. One major challenge with using porphyrin-based PS is their tendency to aggregate in water, which can reduce their effectiveness. To address this issue, considerable research is focused on developing advanced nanostructures that can encapsulate and deliver porphyrin-based PS more effectively, thereby improving their solubility, stability, and selectively for target pathogens.

Detailed structure-activity relationship studies have underscored the critical role of both the CD type and porphyrin substitution patterns in tailoring these conjugates for specific applications. The

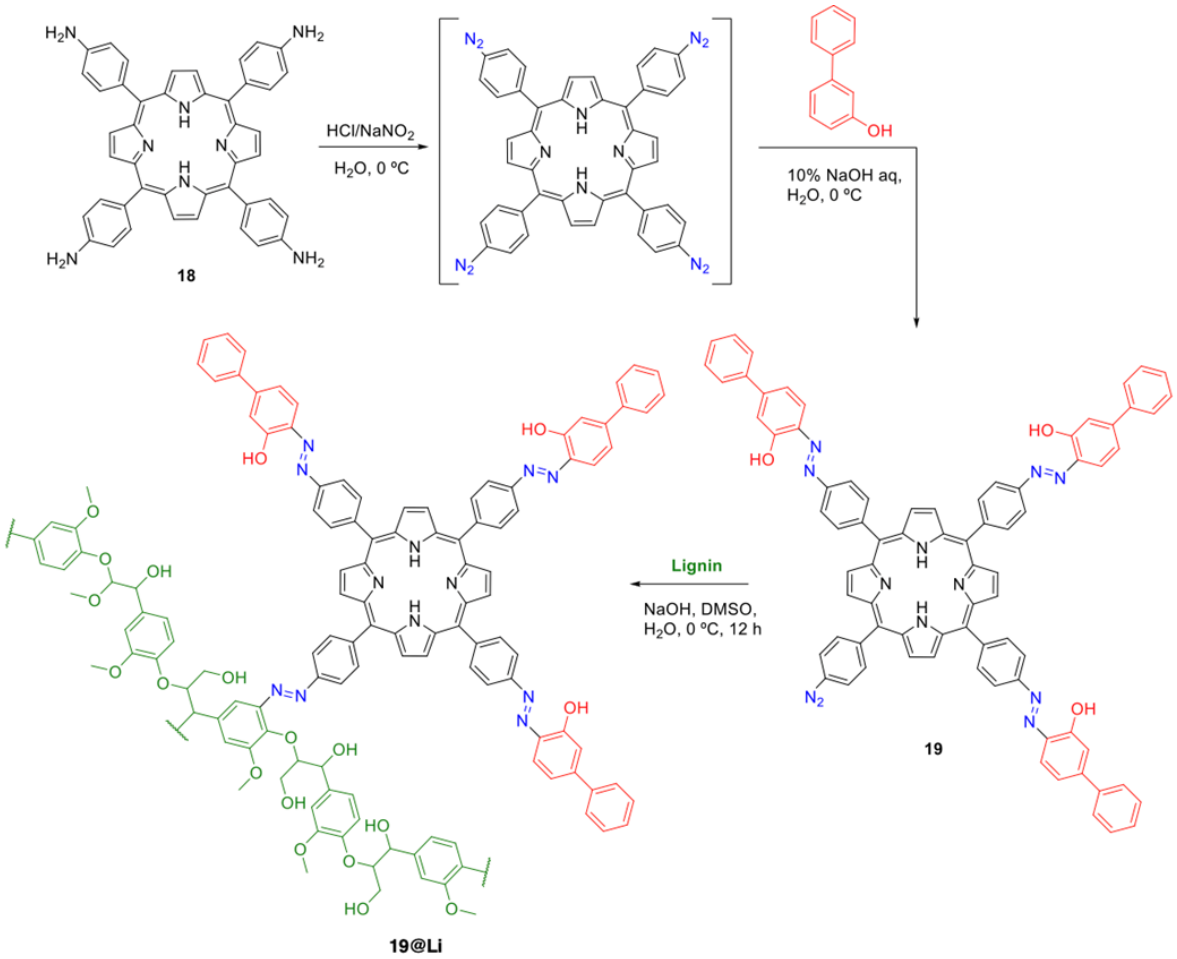

Scheme 8 | Synthetic approach to synthesize **19@Li** NPs considered in the work of Tse *et al.* [52].

formation of functional supramolecular assemblies in aqueous solutions, driven by non-covalent interactions effectively mitigates porphyrin aggregation while enhancing water solubility, resulting in efficient $^1O_2$ generation and improved photostability.

The porphyrin incorporation in CD nanosponges and exploring solvent-free synthetic methodologies further broaden the therapeutic potential of these systems, emphasizing the promise of porphyrin-CD conjugates in a wide range of biomedical applications. The unique benefits of CS are also being actively harnessed in aPDT. CS not only boost the stability and bioavailability of PS, but its inherent antimicrobial properties make it a highly appealing material. Researchers are currently delving into innovative strategies like CS-encapsulated metal-organic nanoparticles, which show promising effectiveness against multidrug-resistant bacteria. These advancements suggest that aPDT utilizing CS could be effective in treating various diseases, including infections and cancer. Additionally, the exploration of lignin-based nanoparticles as innovative carriers for PS has opened exciting new paths in aPDT, particularly against Gram-positive bacterial infections. This approach highlights the potential of using sustainable biomaterials like lignin in the battle against infectious diseases.

In summary, the thoughtful combination of the beneficial properties of biopolymeric materials, such as CD, CS, and Li with the phototherapeutic capabilities of porphyrin derivatives represents a significant and promising direction in developing innovative therapeutic strategies for a wide range of health issues, including bacterial infectious diseases and cancer.

Funding

This research work received financial support from University of Aveiro and Fundação para a Ciência e Tecnologia and Ministério da Ciência, Tecnologia e Ensino Superior (FCT/MCTES) for the financial support of the UID/50006 - Laboratório Associado para a Química Verde - Tecnologias e Processos Limpos unit through national funds. FMP Morais also thanks FCT for his doctoral grant (UI/BD/154486/2022). NMM Moura gratefully acknowledges FCT for an Assistant Research Position under the Individual Scientific Employment Stimulus - 6th Edition (2023. 06495.CEECIND). CL thanks the PROTEOMASS Scientific Society (Portugal) by the funding provided through the General Funding Grant 2024-2025, and by the funding provided to the Laboratory for Biological Mass Spectrometry Isabel Moura (#PM001/2019 and #PM003/2016). C.L. thanks the Royal Society of Chemistry for the Sustainable Laboratory Grants 2023 reference L23-8861107285.

Acknoledgements

The authors thank the University of Aveiro and FCT/MCTES for financial support to UID/50006 - Laboratório Associado para a Química Verde - Tecnologias e Processos Limpos.

References

[1] N. Kashef, Y.-Y. Huang, M.R. Hamblin, Nanophotonics 6 (2017) 853–879. DOI: 10.1515/nanoph-2016-0189

[2] C. Vieira, A.T.P.C. Gomes, M.Q. Mesquita, N.M.M. Moura, M.G.P.M.S. Neves, M.A.F. Faustino, A. Almeida, Front. Microbiol. 9 (2018) 1–16. DOI: 10.3389/fmicb.2018.02665

[3] M. Q. Mesquita, C. J. Dias, M. P. M. S. Neves, A. Almeida, M. F. Faustino, Molecules 23 (2018) 2424. DOI: 10.3390/molecules23102424

[4] M.R. Hamblin, Curr. Opin. Microbiol. 33 (2016) 67–73. DOI: 10.1016/j.mib.2016.06.008

[5] H. Abrahamse, M.R. Hamblin, Biochem. J. 473 (2016) 347–364. DOI: 10.1042/BJ20150942

[6] A.M. Udrea, A. Smarandache, A. Dinache, C. Mares, S. Nistorescu, S. Avram, A. Staicu, Pharmaceutics 15 (2023) 2124. DOI: 10.3390/pharmaceutics15082124

[7] I.S. Mfouo-Tynga, L.D. Dias, N.M. Inada, C. Kurachi, Photodiagnosis Photodyn. Ther. 34 (2021) 102091. DOI: 10.1016/j.pdpdt.2020.102091

[8] R. Baskaran, J. Lee, S.-G. Yang, Biomater. Res. 22 (2018) 25. DOI: 10.1186/s40824-018-0140-z

[9] J.M. Dąbrowski, B. Pucelik, A. Regiel-Futyra, M. Brindell, O. Mazuryk, A. Kyzioł, G. Stochel, W. Macyk, L.G. Arnaut, Coord. Chem. Rev. 325 (2016) 67–101. DOI: 10.1016/j.ccr.2016.06.007

[10] A. Almeida, M.A. Faustino, J.P. Tomé, Future Med. Chem. 7 (2015) 1221–1224. DOI: 10.4155/fmc.15.59

[11] A.N. Hurst, B. Scarbrough, R. Saleh, J. Hovey, F. Ari, S. Goyal, R.J. Chi, J.M. Troutman, J.L. Vivero-Escoto, Int. J. Mol. Sci. 20 (2019) 134. DOI: 10.3390/ijms20010134

[12] N. Malatesti, I. Munitic, I. Jurak, Biophys. Rev. 9 (2017) 149–168. DOI: 10.1007/s12551-017-0257-7

[13] J. Singh, I. Dhamija, H. Meehenian, N. Kumar, S. Simran, M. Muskan, M.L. Verma, S. Kumar, Bull. Natl. Res. Cent. 46 (2022) 202. DOI: 10.1186/s42269-022-00904-y

[14] A. Ikeda, S. Satake, T. Mae, M. Ueda, K. Sugikawa, H. Shigeto, H. Funabashi, A. Kuroda, ACS Med. Chem. Lett. 8 (2017) 555–559. DOI: 10.1021/acsmedchemlett.7b00098

[15] P. Ahmadi, A. Ahmadi, M. Tabibiazar, S. Hamidi, S. Ramezani, Carbohydr. Polym. 353 (2025) 123241. DOI: 10.1016/j.carbpol.2025.123241

[16] L.A. Gusmão, A.E.H. Machado, J.R. Perussi, Photodiagnosis Photodyn. Ther. 40 (2022) 103073. DOI: 10.1016/j.pdpdt.2022.103073

[17] P. Saha, M.R. Rafe, Heliyon 9 (2023) e19287. DOI: 10.1016/j.heliyon.2023.e19287

[18] C.P.S. Ribeiro, M.A.F. Faustino, A. Almeida, L.M.O. Lourenço, Microorganisms 10 (2022) 0–13. DOI: 10.3390/microorganisms10040718

[19] C.P.S. Ribeiro, S.R.D. Gamelas, M.A.F. Faustino, A.T.P.C. Gomes, J.P.C. Tomé, A. Almeida, L.M.O. Lourenço, Photodiagnosis Photodyn. Ther. 31 (2020) 101788. DOI: 10.1016/j.pdpdt.2020.101788

[20] S. Panagiotakis, B. Mavroidi, A. Athanasopoulos, A.R. Gonçalves, L. Bugnicourt-Moreira, T. Regagnon, N. Boukos, G. Charalambidis, A.G. Coutsolelos, M. Grigalavicius, T.A. Theodossiou, K. Berg, C. Ladavière, M. Pelecanou, K. Yannakopoulou, Carbohydr. Polym. 306 (2023) 120579. DOI: 10.1016/j.carbpol.2023.120579

[21] J. Yu, S. Xiao, F. Chen, L. Li, G. Xu, Dye. Pigment. 180 (2020) 108518. DOI: 10.1016/j.dyepig.2020.108518

[22] S.-R. Choi, G.A. Talmon, B.E. Britigan, P. Narayanasamy, ACS Infect. Dis. 7 (2021) 2299–2309. DOI: 10.1021/acsinfecdis.0c00896

[23] S. Shaikh, P.S. Chary, N.K. Mehra, Int. J. Pharm. 671 (2025) 125277. DOI: 10.1016/j.ijpharm.2025.125277

[24] R. Zagami, D. Franco, J.D. Pipkin, V. Antle, L. De Plano, S. Patanè, S. Guglielmino, L. Monsù Scolaro, A. Mazzaglia, Int. J. Pharm. 585 (2020) 119487. DOI: 10.1016/j.ijpharm.2020.119487

[25] D. Franco, R. Zagami, L.M. De Plano, N. Burduja, S.P.P. Guglielmino, L.M. Scolaro, A. Mazzaglia, Molecules 28 (2023). DOI: 10.3390/molecules28062493

[26] R. Zagami, A. Rubin Pedrazzo, D. Franco, F. Caldera, L.M. De Plano, M. Trapani, S. Patanè, F. Trotta, A. Mazzaglia, Int. J. Pharm. 637 (2023). DOI: 10.1016/j.ijpharm.2023.122883

[27] T. Yumoto, S. Satake, S. Hino, K. Sugikawa, R. Kawasaki, A. Ikeda, Org. Biomol. Chem. 18 (2020) 6702–6709. DOI: 10.1039/D0OB01379J

[28] L. Xia, J. Wu, B. Huang, Y. Gao, J. Tian, W. Zhang, Chem. Commun. 56 (2020) 11134–11137. DOI: 10.1039/d0cc03574b

[29] L. Greci, J. Kaczor, P. Carloni, E. Damiani, L. Greci, P. Stipa, F. Tanfani, E. Tartaglini, M. Wozniak, Res. Clwm. Lntermed 19 (1993) 395–405.

[30] S. Qu, X. Ma, S. Yu, R. Wang, Front. Bioeng. Biotechnol. 11 (2023) 1–11. DOI: 10.3389/fbioe.2023.1234758

[31] M. Kołodziejska, K. Jankowska, M. Klak, M. Wszoła, Nanomaterials 11 (2021) 1–44. DOI: 10.3390/nano11113019

[32] B. Sultankulov, D. Berillo, K. Sultankulova, T. Tokay, A. Saparov, Biomolecules 9 (2019) 470. DOI: 10.3390/biom9090470

[33] K.A.D.F. Castro, N.M.M. Moura, F. Figueira, R.I. Ferreira, M.M.Q. Simões, J.A.S. Cavaleiro, M.A.F. Faustino, A.J.D. Silvestre, C.S.R. Freire, J.P.C. Tomé, S. Nakagaki, A. Almeida, M.G.P.M.S. Neves, Int. J. Mol. Sci. 20 (2019) 2522. DOI: 10.3390/ijms20102522

[34] R. Yañez-Macías, A. Muñoz-Bonilla, M.A. De Jesús-Tellez, H. Maldonado-Textle, C. Guerrero-Sánchez, U.S. Schubert, R. Guerrero-Santos, Polymers (Basel). 11 (2019) 1789. DOI: 10.3390/polym11111789

[35] C. Hu, D. Jiang, Y. Zhang, H. Gao, Y. Zeng, N. Khaorapapong, Z. Liu, Y. Yamauchi, M. Pan, Coord. Chem. Rev. 523 (2025) 216264. DOI: 10.1016/j.ccr.2024.216264

[36] D. Tahir, A. Ardiansyah, H. Heryanto, E.E.M. Noor, M.A. Mohamed, Int. J. Biol. Macromol. 298 (2025) 140010. DOI: 10.1016/j.ijbiomac.2025.140010

[37] K.A.D.F. Castro, N.M.M. Moura, A. Fernandes, M.A.F. Faustino, M.M.Q. Simões, J.A.S. Cavaleiro, S. Nakagaki, A. Almeida, Â. Cunha, A.J.D. Silvestre, C.S.R. Freire, R.J.B. Pinto, M. da G.P.M.S. Neves, Dye. Pigment. 137 (2017) 265–276. DOI: 10.1016/j.dyepig.2016.10.020

[38] L.B. Silva, K.A.D.F. Castro, C.E.A. Botteon, C.L.P. Oliveira, R.S. da Silva, P.D. Marcato, Front. Bioeng. Biotechnol. 9 (2021) 1–15. DOI: 10.3389/fbioe.2021.679128

[39] Y. Zhang, J. Ma, D. Wang, C. Xu, S. Sheng, J. Cheng, C. Bao, Y. Li, H. Tian, Biomater. Sci. 8 (2020) 6526–6532. DOI: 10.1039/D0BM01427C

[40] M.S. Hasanin, M. Abdelraof, M. Fikry, Y.M. Shaker, A.M.K. Sweed, M.O. Senge, Molecules 26 (2021). DOI: 10.3390/molecules26123551

[41] C. Musewald, G. Hartwich, F. Pöllinger-Dammer, H. Lossau, H. Scheer, M.E. Michel-Beyerle, J. Phys. Chem. B 102 (1998) 8336–8342. DOI: 10.1021/jp982309z

[42] H.L. Kee, J. Bhaumik, J.R. Diers, P. Mroz, M.R. Hamblin, D.F. Bocian, J.S. Lindsey, D. Holten, J. Photochem. Photobiol. A Chem. 200 (2008) 346–355. DOI: 10.1016/j.jphotochem.2008.08.006

[43] P. Sen, R. Soy, S. Mgidlana, J. Mack, T. Nyokong, Dye. Pigment. 203 (2022) 110313. DOI: 10.1016/j.dyepig.2022.110313

[44] M. Erfani Jazi, G. Narayanan, F. Aghabozorgi, B. Farajidizaji, A. Aghaei, M.A. Kamyabi, C.M. Navarathna, T.E. Mlsna, SN Appl. Sci. 1 (2019) 1–19. DOI: 10.1007/s42452-019-1126-8

[45] E. Csiszár, D. Kun, F. Temesváry-Kis, E. Fekete, Carbohydr. Polym. Technol. Appl. 9 (2025) 100743. DOI: 10.1016/j.carpta.2025.100743

[46] M. Balk, P. Sofia, A.T. Neffe, N. Tirelli, Int. J. Mol. Sci. 24 (2023) 11668. DOI: 10.3390/ijms241411668

[47] G. Marchand, G. Fabre, N. Maldonado-Carmona, N. Villandier, S. Leroy-Lhez, Nanoscale Adv. 2 (2020) 5648–5658. DOI: 10.1039/D0NA00615G

[48] X. Liu, M. Li, X. Li, M. Ge, S. Liu, S. Li, J. Li, J. Ding, A.J. Ragauskas, W. Sun, T.D. James, Z. Chen, Mater. Today Chem. 26 (2022) 101000. DOI: 10.1016/j.mtchem.2022.101000

[49] N. Maldonado-Carmona, G. Marchand, N. Villandier, T.S. Ouk, M.M. Pereira, M.J.F. Calvete, C.A. Calliste, A. Żak, M. Piksa, K.J. Pawlik, K. Matczyszyn, S. Leroy-Lhez, Front. Microbiol. 11 (2020) 1–17. DOI: 10.3389/fmicb.2020.606185

[50] G. Piccirillo, N. Maldonado-Carmona, D.L. Marques, N. Villandier, C.A. Calliste, S. Leroy-Lhez, M.E.S. Eusébio, M.J.F. Calvete, M.M. Pereira, Catal. Today 423 (2023) 113903. DOI: 10.1016/j.cattod.2022.09.009

[51] N. Maldonado-Carmona, T.S. Ouk, N. Villandier, C.A. Calliste, M.J.F. Calvete, M.M. Pereira, S. Leroy-Lhez, Antibiotics 10 (2021) 1–26. DOI: 10.3390/antibiotics10050513

[52] H.Y. TSE, C.S. Yeung, C.Y. Lau, M.Y. Cheung, J. Guan, M.K. Islam, P.T. Anastas, S.Y. Leu, Green Chem. 24 (2022) 2904–2918. DOI: 10.1039/d2gc00196a